Journal of Statistical Physics, Vol. 83, Nos. 5/6, 1996

Bifurcations of an Iterated Mapping with Retardations

W. Götze[1]

Received February 23, 1995; final October 17, 1995

An elementary example for an iterated mapping with retardation is defined, which exhibits a Whitney fold bifurcation of the long-time limit. The long-time dynamics is quite different from the bifurcation scenario known for conventional iterated mappings. There appear two nontrivial power-law exponents, one describing the decay toward a plateau value and the other describing the one below this plateau, which vary continuously with a model parameter. The slowing down of the dynamics near the critical point is ruled by two divergent time scales, characterized by two different nonuniversal exponents. This leads to a stretching of the relaxation over large time intervals. A scaling law description of the bifurcation dynamics is derived.

KEY WORDS: Iterated mappings; dynamics with retardation; bifurcations; nonuniversal power law decay; dynamical scaling laws.

INTRODUCTION

It is well understood that some properties of dynamical systems can be studied also for iterated mappings $\vec{g}_m = \vec{\mathscr{F}}(\vec{\varepsilon}, \vec{g}_{m-1})$, $m = 1, 2, \ldots$.[1] Here $\vec{g}_m$ is some vector in a normed space **B** and $\vec{\mathscr{F}}$ is a non-linear transformation depending smoothly on $\vec{g}_{m-1}$ and on a control parameter vector $\vec{\varepsilon}$. A particular phenomenon of interest is the Whitney fold (or saddle-node) bifurcation of the large-m limit $\vec{g}_m \to \vec{f}$.[2,3] In this case one can choose **B** as the set of real numbers and $\vec{g}_m$, $\vec{\varepsilon}$ as real scalars g_m, ε, respectively. Most naively, one may view this iterated mapping as representing a first-order differential equation where the time is chosen discrete. The mapping

[1] Physik-Department, Technische Universität München, D-85747 Garching; and Max-Planck-Institut für Physik, Werner-Heisenberg-Institut, D-80805 München, Germany.

0022-4715/96/0600-1183$09.50/0

describes the evolution of g_m out of some initial value g_0. In this paper a mapping of real numbers g_m shall be studied,

$$g_m = \mathcal{F}(\varepsilon, g_0, g_1, \ldots, g_{m-1}), \qquad m = 1, 2, \ldots \tag{1}$$

which generalizes the conventional problem in the sense that g_m depends on all preceding values $g_0, g_1, \ldots, g_{m-1}$.

It is a signature of a fold bifurcation that for ε tending toward a critical value ε_c from one side, say $\varepsilon > \varepsilon_c$, the limit f approaches a critical value f_c as a square root law. Choosing $\varepsilon_c = 0$, $f_c = 0$, one gets

$$f = a\sqrt{\varepsilon} + O(\varepsilon), \qquad \varepsilon \to 0+ \tag{2}$$

For small negative ε there is no f near f_c. The model to be studied exhibits the behavior (2). The new results concern the asymptotic dependence of g_m for large m and small ε. These results shall be contrasted with the conventional ones for a fold bifurcation for a nonlinear differential equation. The reader can deduce the conventional results from the elementary evolution equation: $\dot{g}(t) = -g^2(t) + \varepsilon$, $g(t=0) = g_0 > 0$. The discrete version $g_{m+1} = g_m(1 - g_m) + \varepsilon$ of this example was used to discuss the laminar regions for an intermittency problem.[4] For the decay at the critical point one obtains the power law: $g(t \to \infty) \sim (t_0/t)$, $\varepsilon = 0$. The dynamics within a window, where $|g(t) - f_c|$ is small, is described by a scaling law

$$g(t, \varepsilon) = \gamma_\varepsilon g_\pm(t/\tau_\varepsilon), \qquad \varepsilon \gtrless 0. \tag{3}$$

Here the amplitude scale reads $\gamma_\varepsilon \propto |\varepsilon|^{1/2}$ and the time scale follows a related power law: $\tau_\varepsilon \propto 1/\gamma_\varepsilon$. The control parameter independent master functions are: $g_+(\hat{t}) = \coth(\hat{t})$, $g_-(\hat{t}) = \cot(\hat{t})$. The quoted results are universal; they describe the generic fold bifurcation dynamics for all differential equations or mappings no matter how complicated $\mathbf{B}$ or $\mathcal{F}$ might be.

A convincing motivation or obvious physical interpretation for the model (1) to be discussed shall not be given. It is suggested that the model is interesting since it deals with a novel nontrivial scenario. This scenario implies predictions between measurable quantities if one compares the results with correlation functions of glass forming liquids. Some experimental results shall be cited which are compatible with the results derived from (1). These points are explained in more detail in the discussion Section 4. In Section 2 the model is defined. In Section 3 the bifurcation scenario is described in detail.

2. DEFINITION OF THE MODEL

The transformation $\mathscr{T}$ in (1) is given by the elementary expression

$$\mathscr{T} = \{g_0 - [g_0^2 - \lambda(\mathscr{Y}_m - \mathscr{X}_m)]^{1/2}\}/\lambda \tag{4}$$

Here $\mathscr{X}_m$, $\mathscr{Y}_m$ are second order polynomials:

$$\mathscr{X}_m = \mathscr{X}_m(g_1, \ldots, g_{m-1}) = \sum_{l=1}^{m-1} g_{m-l} g_l, \qquad m = 2, 3, \ldots, \mathscr{X}_1 = 0 \tag{5a}$$

$$\mathscr{Y}_m = \mathscr{Y}_m(\varepsilon, g_0, \ldots, g_{m-1}) = (m+1)\,\varepsilon + \lambda \sum_{l=0}^{m-1} g_l^2, \qquad m = 1, 2, \ldots \tag{5b}$$

The initial values shall be restricted to $g_0 > 0$, the number λ to $0 < \lambda < 1$, and the control parameter ε to $\varepsilon < (1-\lambda)\, g_0^2$. This ensures $g_1 < g_0$, where $g_1 = (g_0/\lambda)(1 - \sqrt{W})$; $W = (1-\lambda^2) - (2\varepsilon\lambda/g_0^2)$, $W > 0$.

One can prove the monotony $g_{m+1} < g_m$, $m = 0, 1, \ldots$. Therefore

$$g_0^2 - \lambda(\mathscr{Y}_m - \mathscr{X}_m) > g_0^2 - \lambda(\mathscr{Y}_1 - \mathscr{X}_1) = g_0^2 W$$

Hence, the argument of the square root in (4) has a distance from the branch point not smaller than $g_0^2 W$. Consequently, $\mathscr{T}(\varepsilon, g_0, \ldots, g_{m-1})$ is a real number, depending smoothly on ε, $g_0, \ldots, g_{m-1}$ and λ. In particular, for every fixed m_0 there is some $\varepsilon_0 = \varepsilon_0(m_0) > 0$, so that g_m is analytic in ε for all $|\varepsilon| < \varepsilon_0$ and all $m = 0, 1, \ldots, m_0$. These remarks ensure that Eqs. (4) and (5) define a well-behaved iterated mapping.

Obviously, the sequence g_m solves the infinite set of implicit equations

$$\sum_{l=0}^{m} g_{m-l} g_l = \sum_{l=0}^{m} (\varepsilon + \lambda g_l^2), \qquad m = 1, 2, \ldots \tag{6}$$

Generically, for given $g_0, \ldots, g_{m-1}$ Eq. (6) has two solutions for g_m. If $g_m > -g_0/\lambda$ the solution used in (4) can be obtained as stable fixed point of the iteration procedure

$$g_m^{(r+1)} = [\lambda(g_m^{(r)})^2 + \mathscr{Y}_m - \mathscr{X}_m]/2g_0, \qquad r = 1, 2, \ldots \tag{7}$$

One finds that $g_m^{(r)} \to g_m$ for $r \to \infty$ if $g_m^{(0)}$ is smaller than the unstable fixed point. The latter is given by Eq. (4) with the sign of the root altered to plus.

This observation can be used to define a new iterated mapping as follows. One chooses some fixed $s = 1, 2, \ldots$. One uses (7) with $g_m^{(0)} = g_{m-1}$

to define $g_m^{(r)}$ for $r = 1, 2, ..., sm$. Then one defines $g_m = g_m^{(sm)}$. Obviously, the asymptotic dynamics of the new sequence g_m is the same as the one of the sequence defined by Eqs. (4) and (5). In addition, one notices that one can get the new g_m as close to the old ones as one likes, provided one chooses s sufficiently large. The constructed iterated mapping so will exhibit the same bifurcation as the old one, but avoids the use of square roots; it is defined entirely with polynomials.

3. THE BIFURCATION SCENARIO

The bifurcation for the specified model is illustrated by Figs. 1 and 2. These are evaluated for $g_0 = 10$, $\lambda = 0.7$, $\varepsilon = \pm 4.8/4^n$ with $n = 1, 2, ..., 6$. The g_m are exhibited by symbols for $m = 1, ..., 10$ and by g versus t interpolation curves for $m \geqslant 11$. The following convention has been adopted: $g_m = g(t_m)$, $t_m = (m + 0.5)$.

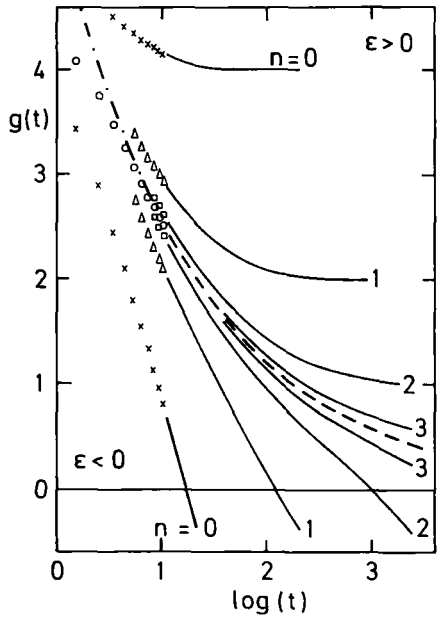

Fig. 1. Results g of the iterated mapping, Eqs. (4) and (5), for $\lambda = 0.7$ and control parameters $\varepsilon = 0$ (dashed line, open circles) and $\varepsilon = \pm 4.8/4^n$: $g_m = g(t_m)$, $t_m = (m + 0.5)$. For $m \leqslant 10$ the g_m are shown by symbols and for $m \geqslant 11$ as interpolation lines. The dashed-dotted line is the critical decay law $g_c = A/t^a$ with $a = 0.327$ and $A = 5.47$.

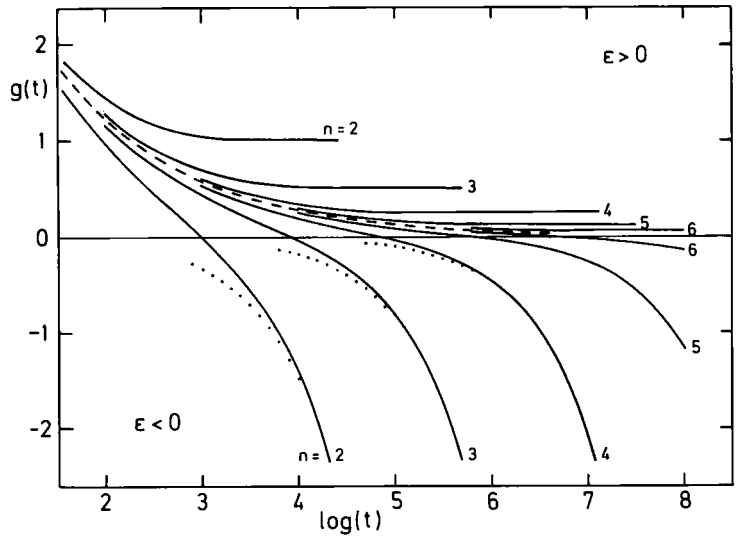

Fig. 2. Results as in Fig. 1, but extended to larger t and bigger n. The dotted lines are the von Schweidler decay laws $g = -B' t^b$ with $b = 0.641$ and B' chosen so that the asymptotes for the curves $\varepsilon < 0$, $n = 2, 3, 4$ are matched for $g < -10$.

3.1. The Bifurcation Parameter f

The monotony $g_{n-1} - g_n \geqslant 0$ ensures that the long time limit $g(t \to \infty) = f$ exists, either as a finite number or as $-\infty$. Subtracting from (6) the same equation with m replaced by $(m-1)$, one gets

$$g_m g_0 = \varepsilon + \lambda g_m^2 + \sum_{l=0}^{m-1} (g_{m-1-l} - g_{m-l})\, g_l$$

and thus $g_m \geqslant 0$ for $\varepsilon \geqslant 0$. If f is finite, one derives from Eq. (6) that $f^2 = \varepsilon + \lambda f^2$. Therefore

$$g(t \to \infty) = f = [\varepsilon/(1-\lambda)]^{1/2}, \qquad \varepsilon \geqslant 0 \tag{8}$$

and g diverges to minus infinity for $\varepsilon < 0$. The value $\varepsilon = 0$ marks a critical point where the long-time limit exhibits a Whitney fold bifurcation, Eq. (2).

3.2. The Critical Decay Law

The decay at the critical point exhibits power-law decrease for large times, specified by some critical exponent a:

$$g(t \to \infty) \sim A/t^a, \qquad \varepsilon = 0, \qquad A > 0 \tag{9}$$

Exponent a decreases monotonically from 1/2 to 0 if λ increases from 0 to 1. The nonuniversality of a is a first remarkable difference of the present model distinguishing it from conventional bifurcation theories. In Figs. 1 and 2 the decay for $\varepsilon = 0$ is shown as a dashed line. The power-law asymptote is exhibited in Fig. 1 as chain a curve for $a = 0.327$. For $t > 120$, this asymptote cannot be distinguished from the solution g for $\varepsilon = 0$ in the figures.

From the mentioned regularity properties of the g_m for finite $m \leqslant m_0$ one concludes here as in conventional theories the following. For every accuracy level $\eta > 0$ one finds two time scales $\tau_{1,2} = \tau_{1,2}(\eta)$. They specify an interval $\tau_1 < t < \tau_2$ for which g agrees with A/t^a within the error η. Within this interval g depends smoothly on ε only, and also τ_1 is a smooth function of ε. Thus for small ε, both g and τ_1 are insensitive functions of the control parameter. The whole sensitive dependence of the dynamics is hidden in the ε dependence of τ_2, delimiting the interval for the critical decay at large times. The window for the critical dynamics expands to arbitrary sizes upon approaching the critical point: $\tau_2 \to \infty$ if $\varepsilon \to 0$.

3.3. The Von Schweidler Law

For negative separation parameters the long-time part follows a power law specified by an exponent, to be denoted by b:

$$g(t \to \infty)/g_0 \sim -(t/\tau_\alpha)^b, \qquad \varepsilon < 0 \tag{10}$$

Exponent b increases monotonically from zero to infinity if λ decreases from 1 to 0. The long-time asymptote (10) depends sensitively on the control parameter ε. This is specified by the ε-dependent scale τ_α; for $\varepsilon \to 0$ one finds $\tau_\alpha \to \infty$. In Fig. 2 the asymptotes (10) are shown with $b = 0.641$ as dotted curves; the τ_α are chosen so as to match the g versus log t curves for $n = 2, 3, 4$ and $g(t) \leqslant g_0$.

Result (10) has no proper counterpart in the theory of fold bifurcations for differential equations or iterated mappings without retardation effects. Indeed, only in the limit $\lambda \to 0$, i.e., $b \to \infty$, do the g versus log t curves look similar to those obtained for conventional theories.

There are two scenarios for the onset of the power law (10). First, the transient dynamics can decrease g to negative values and then the decrease

according to Eq. (10) takes over for larger times. This happens for large $|\varepsilon|$. Figure 1 demonstrates this situation for the $n=0$ result. In this particular case $g(t)$ agrees with the asymptote (10) within 1% for $t>120$, i.e., for $g(t)<-g_0$. Second, after the transient dynamics is ended near some τ_1, the decay follows the critical law (9) till about $\tau_1 \approx \tau_2$. Then $g(t)$ changes sign and crosses over to the asymptote (10). This occurs for small $|\varepsilon|$, as is demonstrated in Fig. 2 for the curve $n=4$. It was discussed carefully by von Schweidler that decay curves in materials, which nowadays are called glassy follow the law (10).[5]

3.4. The Time Scales

A time scale τ_α for the quantification of the long-time dynamics for $\varepsilon<0$ can be defined, for example, by $g(t=\tau_\alpha)=-g_0$. It agrees with the scale entering the von Schweidler law (10) within that accuracy, which allows us to identify g with its long-time asymptote. For small separation parameters $\sigma \propto \varepsilon$ one finds power-law behavior, to be specified by some exponent γ and some control-parameter-insensitive prefactor S_α:

$$\tau_\alpha \sim S_\alpha |\sigma|^{-\gamma}, \qquad \sigma \to 0- \tag{11}$$

Exponent γ increases monotonically from 1 to ∞ if λ increases from 0 to 1. Figure 3 exhibits the τ_α versus σ results obtained from Fig. 2 for $n=2$–5; the line through the data points is the power law (11) for $\gamma=2.31$. The abscissa is labelled with $\sigma=5\varepsilon$.

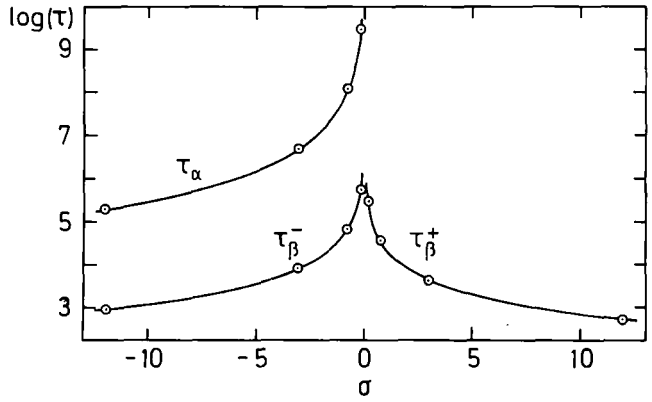

Fig. 3. Time scales τ_α, $\tau_\beta^\pm$ specifying the curves in Fig. 2 for $n=2, 3, 4, 5$. For definitions see text; $\sigma=5\varepsilon$. The lines ar power laws: $1/\tau_\alpha \propto |\sigma|^\gamma$, $1/\tau_\beta^+ \propto 1/\tau_\beta^- \propto |\sigma|^\delta$ with $\gamma=2.31$, $\delta=1.53$ and constants of proportionality chosen such that the $|\sigma|=3$ results are matched.

Scale τ_α has no counterpart for the $\varepsilon > 0$ results, unless one wants to use $\tau_\alpha = \infty$. For those large t, where the $\varepsilon < 0$ results follow Eq. (10), the $\varepsilon > 0$ results have reached the time-independent plateau f from Eq. (8). Thus one can characterize the slowing down of the dynamics as follows. Upon increasing the control parameter ε toward the critical point 0, the decay rate $\omega_\alpha = 2\pi/\tau_\alpha$ decreases to zero: $\omega_\alpha \propto |\varepsilon|^\gamma$. For $\varepsilon > 0$ one finds arrest: $\omega_\alpha = 0$.

Another scale specifying the slow dynamics for $\varepsilon < 0$ can be defined by the zero of the decay function. It shall be denoted by τ_β^-: $g(t = \tau_\beta^-) = 0$. A scale quantifying the slow dynamics for $\varepsilon > 0$ can be introduced as that time where g reaches the plateau within, say, 10%: $g(t = \tau_\beta^+) = 1.1f$. Both scales $\tau_\beta^\pm$ exhibit power-law divergences at the critical point specified by control-parameter-insensitive prefactors $S_\beta^\pm$ and a common exponent, denoted by δ:

$$\tau_\beta^\pm \sim S_\beta^\pm |\sigma|^{-\delta}, \qquad \sigma \to 0\pm \tag{12}$$

Again, δ increases monotonically from 1 to ∞ if λ increases from 0 to 1. Figure 3 exhibits the results from Fig. 2 for $n = 2$–5; and the full lines show the power laws (12) for $\delta = 1.53$.

The cusplike shape of the $\tau_\beta^\pm$ versus σ plot is qualitatively similar to what one finds for conventional bifurcations. τ_β is the analog of the scaling time τ_ε of the conventional result (3). The dynamics within the windows around $\tau_\beta^\pm$ slows down symmetrically for $|\varepsilon| \to 0$, up to some ε-insensitive amplitude ratio S_β^+ / S_β^-. While the conventional theory implies a universal scale exponent $\delta = 1/2$, the present model implies nonuniversality of the exponent δ; in particular, one can get δ as large as desired.

Since $\gamma > \delta$, one finds the ratio of the scales to diverge:

$$\tau_\alpha / \tau_\beta^- \to \infty, \qquad \sigma \to 0- \tag{13}$$

In this sense one can say that the slowing down of the dynamics upon increasing σ toward the bifurcation point is characterized by two scales. The decay outside the transient regime is a two-step process. The first step is the critical decay toward the plateau. This step extends up to the large times $\tau_\beta^\pm$; these scales are proportional to the time $\tau_2(\eta)$ mentioned in Section 3.2. The second step for $\sigma < 0$ is the decay below the plateau characterized by the even larger scale τ_α. This phenomenon has no analog for conventional Whitney fold bifurcations. Only in the limit $\lambda \to 0$ does one find $\tau_\alpha / \tau_\beta \to 1$, so that the two-step feature disappears. It was explained in Section 3.3 that there are two scenarios for the onset of the long time decay for $\varepsilon < 0$. The two steps occur only for the second scenario, since it

is connected with the appearance of a diverging scale τ_β^-. For the first scenario both scales τ_β^- and τ_α are very close to each other and they do not exhibit sensitive dependences on ε.

3.5. The Amplitude Scale

Upon decreasing $|\varepsilon|$, the g versus log t curves in Fig. 2 are squeezed toward the abscissa. This feature shall be quantified by some amplitude scale C_σ. For $\varepsilon > 0$ one can characterize the size of g by its long time asymptote f in Eq. (8), so that $C_\sigma \propto |\sigma|^{1/2}$. For $\varepsilon < 0$ the amplitude shall be quantified by the slope χ of the g versus log t graph at the zero:

$$\chi = -dg(t)/d\log(t), \qquad t = \tau_\beta^-, \qquad \varepsilon < 0 \tag{14}$$

One finds the universal $|\sigma|^{1/2}$ law, characterizing Whitney fold bifurcations: $\chi \propto C_\sigma$, where the constant of proportionality depends smoothly on λ. These findings are illustrated in Fig. 4, which is similar to what one gets in conventional theories from Eq. (3).

Within the intermittency theory the length Δt of the laminar region was considered and found to diverge with a universal exponent $\nu = \frac{1}{2}$: $\Delta t \propto 1/|\varepsilon|^{\nu}$.[4] The region extends around the zero τ_β^- where $|g(t)| < \eta_0$ for small η_0. From (14) one derives $\Delta t = \eta_0 \tau_\beta^- / \chi$, so that the present model yields an exponent $\nu = \frac{1}{2} + \delta$.

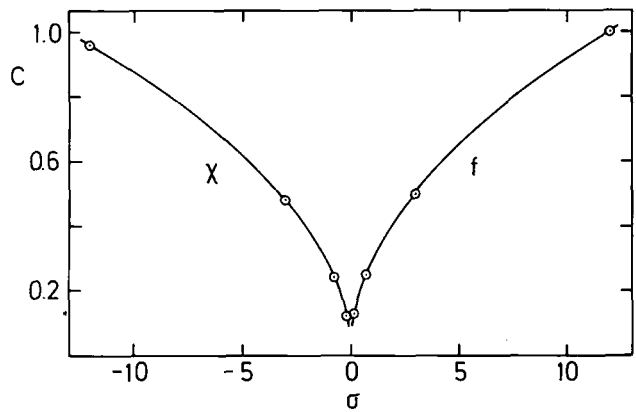

Fig. 4. Correlation scales χ and f as defined in the text, $\sigma = 5\varepsilon$. The curves are square-root laws $f \propto \chi \propto |\sigma|^{1/2}$ with constants of proportionality chosen such that the $|\sigma| = 3$ results are matched.

3.6. The Scaling Laws

Let us examine whether the long-time dynamics follows a scaling law (3), as suggested by the conventional theory. The scales in (3) can be altered by constants and some conventions shall be used to fix various prefactors. The function g_+ has to approach a positive value for large time and here we choose the convention

$$g_+(\hat{t} \to \infty) = 1/(1-\lambda)^{1/2} \tag{15}$$

Then Eq. (8) implies

$$\gamma_\varepsilon = |\varepsilon|^{1/2} \tag{16}$$

In (3) the limit $\varepsilon \to 0$ for fixed t is equivalent to $t \to 0$ for fixed ε, i.e., with (9): $g_\pm(\hat{t} \to 0) \propto 1/t^a$. We choose the convention

$$g_\pm(\hat{t} \to 0) \sim 1/\hat{t}^a \tag{17}$$

Thus one gets from (3), (9)

$$\tau_\varepsilon = A^{1/a}/|\varepsilon|^{1/2a} \tag{18}$$

Von Schweidler's law implies

$$g_-(\hat{t} \to \infty) \sim -B\hat{t}^b \tag{19}$$

The positive parameter B cannot be determined analytically; it follows from matching the long-ime solution to the behavior for intermediate times. Thus one gets for the scale in (10): $\gamma_\varepsilon B/\tau_\varepsilon^b = 1/\tau_\alpha^b$. Since $\tau_\varepsilon \propto \tau_\beta^{\pm}$, one obtains for the two scale exponents δ, γ in (11), (12)

$$\delta = \frac{1}{2a}, \qquad \gamma = \frac{1}{2a} + \frac{1}{2b} \tag{20}$$

The numerical results quoted in connection with Figs. 2 and 3 exemplify these finding.

If $g_m \sim D_\rho m^\rho$ for large m, one can use Euler's formula to obtain for $\rho > -0.5$ the asymptotic expressions

$$\sum_{l=0}^{m} g_l^2 \sim D_\rho^2 m^{2\rho+1}/(2\rho+1)$$

and

$$\sum_{l=0}^{m} g_{m-l} g_l \sim D_\rho^2 m^{2\rho+1} \Gamma(1+\rho)^2/[(2\rho+1)\,\Gamma(1+2\rho)]$$

Here Γ denotes the gamma function. Substitution of these formulas with $\rho = -a, b$ into (6) yields

$$\Gamma(1-a)^2/\Gamma(1-2a) = \lambda = \Gamma(1+b)^2/\Gamma(1+2b) \tag{21}$$

This formula explains the numerical value for the exponents a, b and their variation with λ cited above.

Figure 5 demonstrates the scaling law (3) for those data of Figs. 1 and 2 which deal with the dynamics outside the transient regime. Since the shown numerical results refer to $\gamma_\varepsilon \propto 1/2^n$, the vertical axis in Fig. 5 is chosen such that $\hat{g} = 2^{n-4}g$. Similarly, the time is scaled onto the one for $n=4$: $\hat{t} = t\tau^{(4)}/\tau^{(n)}$. Here $\tau^{(n)}$ is the time τ_β^- introduced in Section 3.4. The rescaling of the time is done trivially in the semilogarithmic plots used in Figs. 1, 2, and 5: one merely carries out a shift of the plot parallel to the abscissa so that the zero of the curve falls on that for the $\varepsilon < 0$, $n=4$ result. Within the accuracy of the drawing all results collapse for $t > 50$ on common curves, which are the master functions $g_\pm$ in some convention for the scales. These functions agree with the result for $n=5$ for the shown 6.25-decade window.

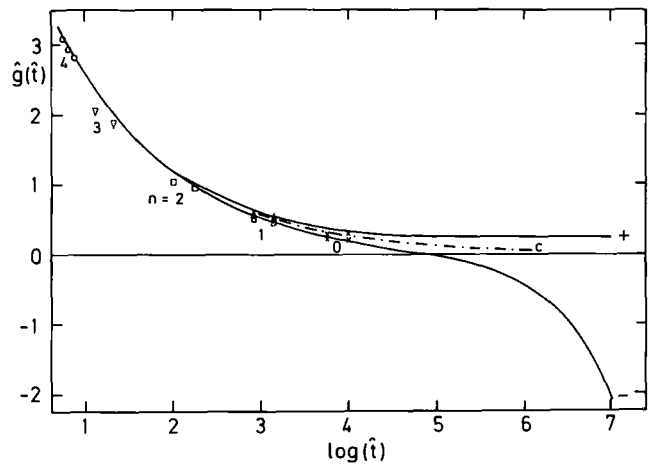

Fig. 5. Decay curves from Figs. 1 and 2 rescaled for each n on the curves for $n=4$ according to $\hat{g} = g2^{4-n}$, $\hat{t} = t\tau^{(4)}/\tau^{(n)}$, where $\tau^{(n)}$ equals τ_-^β for the curve $\varepsilon = -4.8/4^n$; The three open circles are the results for $n=4$ for the points $m=8, 9, 10$, and the other symbols refer to the corresponding points of Fig. 1 for $m=9, 10$. The dashed-dotted line is the critical decay A/t^a, continuting the corresponding curve form Fig. 1. The curves with $\pm$ are the master functions $g_\pm(\hat{t})$ in the scaling law (3); they agree with the rescaled results for $n=5, 6$ within the shown dynamical window.

4. DISCUSSION

The described bifurcation scenario has been discussed before within the so-called mode coupling theory (MCT) for structural relaxation in simple liquids. This theory deals with a regular non-linear model for the calculation of the correlation functions $\phi_k(t)$ for density fluctuations of wave vector k. The MCT exhibits a fold bifurcation for the Debye–Waller factor. A generalization of the center manifold theorem has been proven, yielding $\phi_k(t) = f_k^c + h_k G(t)$. This formula describes the dynamics within a window, where $\phi_k(t) - f_k^c$ is small. The wavevector dependent constants f_k^c, h_k depend smoothly on control parameters. The sensitive dependence of the dynamics enters via a separation parameter σ; it depends smoothly on the system parameters such as the temperature, and its zero defines the critical point. The k-independent function $G(t)$ obeys for large times t the equation

$$(d/dt) \int_0^t G(t-t')\, G(t')\, dt' = \lambda G(t)^2 + \sigma \tag{22}$$

From (22) together with some mathematical assumptions the scaling laws of Section 3 were derived. For details and references to the original literature the reader is referred to the review in ref. 6. Even though the general MCT equations of motion are motivated within the standard theory of liquids, it was not possible to give an ad hoc motivation or physical interpretation for Eq. (22).

The results indicated earlier suggest that there is a whole class of models leading to the bifurcation scenario of Section 3. In the literature it has been left open whether Eq. (22) has a solution. Neither was it possible to specify the conditions which fix the solution of (22) uniquely. In Appendix A it is shown that the asymptotic solutions of the model of Section 2 solve Eq. (22). This model presents therefore the first mathematically well defined example showing that retardation effects can yield a fold bifurcation dynamics which is completely different from what one knows for conventional theories. In this paper a whole series of non-obvious relations for properties of relaxation functions has been obtained. It is suggested to leave it to the experimentalist to work out an assessment of the theory by comparing the various predicted relations with the data.

Von Schweidler's finding[5] has been confirmed repeatedly, typically for dynamical window of 1.5 to 2 decades. A particularly impressive example was found recently in molecular dynamics studies for a supercooled binary mixture of Lennard-Jones atoms.[7] In this case the dynamical window for the von Schweidler decay extended up to three decades and the large signal-to-noise ratio allowed the determination of exponent $b \approx 0.49$ within $\pm 3\%$. The relaxation data for liquids are not compatible with the assumption that exponent b is universal and in all cases the scale τ_α in (10)

depends sensitively on control parameters such as the temperature or density[6]. These findings are reflected by the results (11), (21). In addition, it is predicted that the von Schweidler decay is preceded by another power law decay (9). Its amplitude should be control parameter insensitive and its exponent a can be evaluated from exponent b via Eq. (21). In particular, $a \leqslant 1/2$ is predicted. Fourier transformation leads to a self-similar spectrum $g''(\omega) \propto 1/\omega^{1-a}$. A spectrum with this signature was observed in liquid $0.4Ca(NO_3)_2\ 0.6K(NO_3)$. Neutron scattering experiments detected this spectrum as a large enhancement of the cross section above the white noise level for a frequency window of almost two decades.[8] The spectrum did not show a dependence on wave vector k if the latter was varied between $0.2\ \text{Å}^{-1}$ and $2\ \text{Å}^{-1}$. Polarized and depolarized light scattering experiments detected the critical spectrum with a very good signal-to-noise ratio over a window of almost three decades.[9] In this case the dynamics was probed on length scales which are three orders of magnitude larger than the ones probed in the neutron scattering work. The data yield $a \sim 0.3$. Complete tests of the scaling laws and of the various power laws and their interrelations have been done for the mentioned molten salt mixture[10] and also for colloidal suspensions.[11] In particular, the results on the two scales, as summarized in Fig. 3, had been verified. Thus one can conclude that there are physical systems which follow the dynamical scenario discussed in this paper.

The Fourier transforms $g''_{\pm}(\omega)$ of the master functions $g_{\pm}(\hat{t})$ describe the crossover from the critical decay ω^{-1+a} for $\omega\tau_\varepsilon \gg 1$ to respectively white noise ω^0 or von Schweidler spectra $(\omega\tau_\alpha)^{-1-b}$ for $\omega\tau_\varepsilon \ll 1$. To grasp these stretched spectra one has to scan dynamical windows of three-to four-order-of-magnitude frequency variation. In order to evaluate the predicted spectra numerically with an accuracy of, say 1%, one needs the master functions $g_{\pm}(\hat{t})$ for time intervals extending up to about 10^8. The effort to evaluate g_m is determined by the effort to evaluate $\mathcal{X}_m$ in (5a), i.e., it increases proportional to m^2. However, one can apply a decimation procedure for the iterated mapping as explained in Appendix B. This procedure leaves the equations invariant and reduces the numerical work very efficiently, so that the effort increases proportional to $\ln(m)$ only.

APPENDIX A. THE SCALING EQUATION

Let us define a left continuous decreasing function $g(t) = g(g_0; t, \varepsilon)$ by

$$g(t) = g_l, \qquad l < t \leqslant l+1, \qquad l = 0, 1, \ldots. \tag{A.1}$$

Because of (6) it obeys the non-linear integral equation

$$\int_0^t g(t-t')\, g(t')\, dt' = \int_0^t (\lambda g(t')^2 + \varepsilon)\, dt' \tag{A.2}$$

for all $t=(m+1)$, $m=1, 2,\ldots$. A new function $G_q(t)=G_q(t;\sigma)$ shall be introduced for all $q=1, 2,\ldots$ by rescaling with two parameters $\mu>0$, $\nu>0$ as follows: $G_q(t/\nu q)=\mu g(g_0 q^a, t, \sigma)$; $\sigma=\mu^2\varepsilon$. Obviously, the iterated mapping (5) implies $g(g_0 x; t, \varepsilon)=x g(g_0; t, \varepsilon/x^2)$ and thus $G_q(t/\nu q)=\mu q^a g(g_0; t, \sigma/q^{2a})$. From (A.2) one gets therefore

$$\int_0^t G_q(t-t')\, G_q(t')\, dt' = \int_0^t [\lambda G_q(t')^2 + \sigma]\, dt'; \qquad t=(m+1)/(\nu q) \tag{A.3}$$

For fixed t the limit of large q is determined by g_m for large m. If the latter obeys the scaling law of Section 3.6, there exists $\lim_{q\to\infty} G_q(t)=G(t)$. The latter obeys (A.3) for all times t which are rational multiples of $1/\nu$. Since these numbers are dense, (A.3) is valid for all t, and differentiation yields (22). Up to redefinition of scales, which is possible because the parameters μ and ν can be altered, the function G is given by the master functions

$$g_\pm: \quad G(t,\sigma)=s_1 |\sigma|^{1/2} \cdot g_\pm(s_2 t\, |\sigma|^{1/2a}); \qquad s_1, s_2>0, \quad \sigma \gtrless 0$$

APPENDIX B. A DECIMATION TRANSFORMATION

Equation (6) can be rewritten as

$$2g_0 g_m + \mathscr{X}_m = \lambda g_m^2 + \mathscr{Y}_m \tag{B.1a}$$

$$\mathscr{Y}_m = \varepsilon + \lambda g_{m-1}^2 + \mathscr{Y}_{m-1} \tag{B.1b}$$

For given $g_0,\ldots, g_{m_d-1}$ and $\mathscr{Y}_{m_d}$ these equations determine g_m for $m=m_d,\ldots, m_0$. Definition (5a) has to be observed and the root of (B.1a) has to be chosen as specified in (4).

The number m_0 shall be used as the decimation block size, which is written as $k\cdot m_d$, with some fixed decimation factor $k=2$ or $3,\ldots$. Let us introduce m_d averages

$$\bar{g}_{\bar{m}} = \frac{1}{k}\sum_{l=0}^{k-1} g_{\bar{m}k+l}, \qquad \bar{m}=0, 1,\ldots, m_d-1 \tag{B.2a}$$

and also the number

$$\bar{\mathscr{Y}}_{m_d} = \varepsilon + \frac{1}{k}(\mathscr{Y}_{m_0}-\varepsilon) \tag{B.2b}$$

It shall be assumed that $(m_d/2)$ is chosen so large that coarse graining over blocks of size k is possible for $m \geqslant m_d/2$. This means that within a prescribed accuracy

$$g_{\bar{m}k+l} \approx \bar{g}_{\bar{m}}, \qquad l=0, 1,..., k-1, \quad \bar{m} \geqslant m_d/2 \tag{B.3}$$

where $\bar{g}_{\bar{m}}$ denotes a coarse grained-value. If one applies this formula to Eq. (6) for $m=(\bar{m}+1)k-1$, one arrives at the same set of equations (B.1a), (B.1b), and (5a); however, all quantities carry a bar. Consequently the original equations can be used to evaluate $\bar{g}_{\bar{m}}$ for $\bar{m}=m_d,..., m_0$. Iteration of the procedure R times provides the function $g(t)$ up to $t=m_0 k^R$; the calculation effort increases proportional to $m_0^2 \cdot (R+1)$.

In order to produce the shown figures one can choose $m_0=120$, $k=10$. Choosing $m_0=10^4$, one can read off all quoted exponents with five relevant digits and evaluate spectra $g''(\omega)$ with a relative accuracy not worse than 10^4.

REFERENCES

1. E. Ott, *Chaos in Dynamical Systems* (Cambridge University Press, Cambridge, 1993).
2. J. Guckenheimer and Ph. Holms, *Nonlinear Oscillations, Dynamical Systems, and Bifurcations of Vector Fields* (Springer-Verlag, New York, 1986).
3. V. I. Arnold, *Catastrophe Theory* (Springer-Verlag, Berlin, 1986).
4. P. Manneville and Y. Pomeau, *Physica* **1D**:219 (1980).
5. E. von Schweidler, *Ann. Phys.* **24**:711 (1907).
6. W. Götze and L. Sjögren, *Rep. Prog. Phys.* **55**:241 (1992).
7. W. Kob and H. C. Andersen, *Phys. Rev. Lett.* **73**:1376 (1994).
8. W. Knaak, F. Mezei, and B. Farago, *Europhys. Lett.* **7**:529 (1988).
9. N. J. Tao, G. Li, and H. Z. Cummins, *Phys. Rev. Lett.* **66**:1334 (1991).
10. G. Li, W. M. Du, X. K. Chen, H. Z. Cummins, and N. J. Tao, *Phys. Rev. A* **45**:3867 (1992).
11. W. van Megen and S. M. Underwood, *Phys. Rev. Lett.* **70**: 2766 (1993); *Phys. Rev. E* **49**:4206 (1994); *Phys. Rev. Lett.* **72**:1773 (1994).